Monthly Notices
of the
ROYAL ASTRONOMICAL SOCIETY

MNRAS **442,** 821–837 (2014) doi:10.1093/mnras/stu916

Probing modified gravity theories with ISW and CMB lensing

D. Munshi,[1]⋆ B. Hu,[2] A. Renzi,[3,4] A. Heavens[5] and P. Coles[1]

[1]*Astronomy Centre, School of Mathematical and Physical Sciences, University of Sussex, Brighton BN1 9QH, UK*
[2]*Instituut-Lorentz Theoretical Physics, Universiteit Leiden, Niels Bohrweg 2, 2333 CA Leiden, the Netherlands*
[3]*Department of Mathematics, University of Rome Tor Vergata, Via della Ricerca Scientifica 1, I-00133 Rome, Italy*
[4]*INFN, Sezione di Roma Tor Vergata, Via della Ricerca Scientifica 1, I-00133 Rome, Italy*
[5]*Imperial Centre for Inference and Cosmology, Department of Physics, Imperial College, Blackett Laboratory, Prince Consort Road, London SW7 2AZ, UK*

Accepted 2014 May 6. Received 2014 May 4; in original form 2014 March 4

ABSTRACT

We use the optimized skew-spectrum as well as the skew-spectra associated with the Minkowski functionals to test the possibility of using the cross-correlation of the integrated Sachs–Wolfe effect (ISW) and lensing of the cosmic microwave background (CMB) radiation to detect deviations in the theory of gravity away from General Relativity (GR). We find that the although both statistics can put constraints on modified gravity, the optimized skew-spectra are especially sensitive to the parameter B_0 that denotes the *Compton wavelength* of the scalaron at the present epoch. We investigate three modified gravity theories, namely the post-parametrized Friedmann formalism; the Hu–Sawicki model and the Bertschinger–Zukin (BZ) formalism. Employing a likelihood analysis for an experimental setup similar to ESA's *Planck* mission, we find that, assuming GR to be the correct model, we expect the constraints from the first two skew-spectra, $S_\ell^{(0)}$ and $S_\ell^{(1)}$, to be the same: $B_0 < 0.45$ at 95 per cent confidence level (CL) and $B_0 < 0.67$ at 99 per cent CL in the BZ model. The third skew-spectrum does not give any meaningful constraint. We find that the optimal skew-spectrum provides much more powerful constraint, giving $B_0 < 0.071$ at 95 per cent CL and $B_0 < 0.15$ at 99 per cent CL, which is essentially identical to what can be achieved using the full bispectrum.

Key words: methods: analytical – methods: numerical – methods: statistical – dark energy.

1 INTRODUCTION

The observations of Type Ia supernovae imply that our Universe is undergoing a phase of accelerated expansion (Reiss et al. 1998; Perlmutter et al. 1999). Cosmic acceleration can arise from either an exotic form of energy with negative pressure, referred to as 'dark energy', or a modification of gravity manifesting on large scales. As shown by various authors (Bertschinger 2006; Song, Hu & Sawicki 2007a; Brax et al. 2008; Hu et al. 2013c), determining the cause of the acceleration is hampered by the fact that the background dynamics in dark energy and modified gravity models are nearly indistinguishable. To lift this degeneracy, one can test the evolution of perturbations in these models. The perturbative approach to growth of structure in modified gravity can, in principle, be classified in two different frameworks: parametric and non-parametric, an example of the latter being principal component analysis (Zhao et al. 2009a,b, 2010; Hojjati et al. 2012a). In this paper, we focus on the former.

There exist several phenomenological parametrizations of modified gravity including the Bertschinger–Zukin (Bertschinger & Zukin 2008) parametrization, and that of Starobinsky (2007). These parametrizations are suitable for the quasi-static regime, where the time evolution of the gravitation potentials is negligible compared with their spatial gradient. Furthermore, if we focus on the linear fluctuation dynamics for which the equations in Fourier space can be reduced to simple algebraic relations, these techniques allow us to perform some analytic calculations which make the parametrization technically efficient. However, if we want to go further beyond the quasi-static scale, while remaining in the linear perturbation framework, the parametrization of modified gravity becomes more complex. This is because on the largest scales, especially the super- or near-horizon scales, the time evolution of the gravitational potentials is no longer negligible. In fact, the time derivative terms dominate the dynamical equations, which means that we need to solve some temporal ordinary differential equations. All in

⋆ E-mail: Dipak.Munshi@astro.cf.ac.uk

all, the inclusion of time derivative terms makes the parametrization of modified gravity not so manifest anymore. Actually, there exists some debate about the range of validity of the various parametrizations; on the one hand, as shown by Zuntz et al. (2012), using a parametrization with insufficient freedom significantly tightens the apparent theoretical constraints. On the other hand, for some specific modified gravity models, some phenomenological parametrizations work quite well; for instance, Hojjati et al. (2012b) recently demonstrated that for small Compton wavelength in the $f(R)$ model, the Bertschinger–Zukin parametrization is in practice good enough for current data analysis. This is because, for small Compton wavelengths, the most significant modifications w.r.t. GR occur in the sub-horizon regime, while the modification on the super-horizon scales are subdominant. In addition to the above explicit parametrizations, some quite generic frameworks have been proposed, such as the parametrized post-Friedmann (PPF) formalism, including the Hu–Sawicki approach (Hu & Sawicki 2007b; Fang, Hu & Lewis 2008), its calibration version (Lombriser, Yoo & Koyama 2013) and Baker–Ferreira–Skordis–Zuntz algorithm (Baker et al. 2011; Baker, Fereira & Skordis 2013), and the effective field theory (EFT) formalism (Bloomfield et al. 2012; Gubitosi, Piazza & Vernizzi 2013; Hu et al. 2013c). These formalisms are devoted to build up a 'dictionary' of modified gravity theories and their PPF or EFT correspondence. Since the purpose of these generic formalisms is to construct a unified way to include all the modified gravity/dark energy models, they contain more arbitrary functions/coefficients, which usually lead to looser constraints.

Besides the recent progress on the construction of parametrizations, many observational windows have recently been proposed, such as the integrated Sachs–Wolfe (ISW) effect (Sachs & Wolfe 1967) in cosmic microwave background (CMB) anisotropies (Zhang 2006; Song, Peiris & Hu 2007b; Ho et al. 2008), the power spectrum of luminous red galaxies (Yamamoto et al. 2010; He 2012; Abebe, de la Cruz-Dombriz & Dunsby 2013), cluster abundance (Jain & Zhang 2008; Schmidt, Vikhlinin & Hu 2009; Ferraro, Schmidt & Hu 2011; Lombriser et al. 2012), Coma cluster (Terukina et al. 2014), galaxy peculiar velocities (Li et al. 2013), redshift-space distortions (Jennings et al. 2012; Raccanelli et al. 2013), weak lensing (Heavens, Kitching & Verde 2007; Zhang et al. 2007; Hirata et al. 2008; Daniel et al. 2010; Reyes et al. 2010; Tereno, Semboloni & Schrabback 2011; Laszlo et al. 2012; Simpson et al. 2013), 21 cm observations (Hall, Bonvin & Challinor 2013), matter bispectrum (Marin et al. 2011; Bartolo et al. 2013), etc. In addition, recently some N-body simulation algorithms in modified gravity models have been developed (Li, Mota & Barrow 2011; Zhao, Li & Koyama 2011). As shown by Song et al. (2007b) and Lombriser et al. (2012), with *Wilkinson Microwave Anisotropy Probe* (*WMAP*) resolution the modification effects on the CMB mainly come from the ISW effect, which becomes prominent on the super-horizon scales. However, due to the unavoidable cosmic variance on large scales, the constraints from these effects are not significant. On the other hand, since the typical modification scales are on sub-horizon scales, several studies show that the most stringent constraints come from the large-scale structure data sets. For example, the strongest current constraint on $f(R)$ gravity [$\log_{10}B_0 < -4.07$; 95 per cent confidence level (CL)] (Dossett, Hu & Parkinson 2014) is driven by the galaxy spectrum from WiggleZ data sets (Parkinson et al. 2012). Various previous results show that the main constraint on modified gravity comes from galaxy or cluster scales which corresponds to the multipole range $\ell \gtrsim 500$ in CMB data, where lensing effects are no longer negligible. The recent release of *Planck* data (Planck Collaboration 2013a) provides us with a fruitful late-time information both on ISW and lensing, which is encoded in the CMB temperature power spectrum (Planck Collaboration 2013b), the lensing potential power spectrum (Planck Collaboration 2013c) and the CMB temperature ISW-lensing bispectrum (Planck Collaboration 2013d,e). The full-sky lensing potential map has been constructed and the amplitude of the lensing potential power spectrum has been estimated at the 25σ level. The ISW–lensing bispectrum is also detected with nearly 3σ CL. Although the ISW–lensing bispectrum data have not yet been released, forecasts of constraints on modified gravity models through this novel observational statistic have been investigated (DiValentino 2012; Hu et al. 2013a). These studies show that the ISW-lensing bispectrum is an effective tool to constrain modified gravity. Also notice that Hu et al. (2013b) analysed CMB temperature power-spectrum data alone and improved the previous constraint from *WMAP*9's $B_0 < 3.37$ at 95 per cent CL to $B_0 < 0.91$. Inclusion of the lensing potential power spectrum improved it to $B_0 < 0.12$. The lensing-ISW bispectrum is known to be uncorrelated to the power spectrum and thus it can further tighten the constraint on B_0.

Inspired by these results, in this paper, we use the recently introduced optimum skew-spectra and the skew-spectra associated with the Minkowski functionalss (MFs) to constrain departures from GR. Since their introduction in cosmology by Mecke, Buchert & Wagner (1994), MFs have been extensively developed as a statistical tool for non-Gaussianity in a cosmological setting for both two-dimensional (2D, projected) and three-dimensional (redshift) surveys. Analytic results are known for certain properties of the MFs of a Gaussian random field making them suitable for identifying non-Gaussianity. Examples of such studies include CMB data (Schmalzing & Górski 1998; Novikov, Schmalzing & Mukhanov 2000; Hikage et al. 2008b; Natoli et al. 2010), weak lensing (Matsubara & Jain 2001; Sato et al. 2001; Taruya et al. 2002; Munshi et al. 2012b), large-scale structure (Gott, Mellot & Dickinson 1986; Coles 1988; Gott et al. 1989, 1990; Melott 1990; Gott et al. 1992; Moore et al. 1992; Canavezes et al. 1998; Sahni, Sathyaprakash & Shandarin 1998; Schmalzing & Diaferio 2000; Kerscher et al. 2001; Hikage et al. 2002, 2008a; Park et al. 2005; Hikage, Komatsu & Matsubara 2006), 21 cm (Gleser et al. 2006), frequency-cleaned Sunyaev–Zel'dovich (SZ) maps (Munshi et al. 2013b) and N-body simulations (Schmalzing & Diaferio 2000; Kerscher et al. 2001). The MFs are spatially defined topological statistics and, by definition, contain statistical information of all orders in the moments. This makes them complementary to the poly-spectra methods that are defined in Fourier space. It is also possible that the two approaches will be sensitive to different aspects of non-Gaussianity and systematic effects, although in the weakly non-Gaussian limit it has been shown that the MFs reduce to a weighted probe of the bispectrum (Hikage et al. 2006).

The skew-spectrum is a weighted statistic that can be tuned to a particular form of non-Gaussianity, such as that which may arise either during inflation at an early stage or from structure formation at a later time. The skew-spectrum retains more information about the specific form of non-Gaussianity than the (one-point) skewness parameter alone. This allows not only the exploration of primary and secondary non-Gaussianity but also the residuals from galactic foreground and unresolved point sources (PS). The skew-spectrum is directly related

to the lowest order cumulant correlator and is also known as the two-to-one spectra in the literature (Cooray 2001). In a series of recent publications, the concept of skew-spectra was generalized to analyse the morphological properties of cosmological data sets or in particular the MFs (Munshi et al. 2012b, 2013b,c; Pratten & Munshi 2012). The first of these three spectra, in the context of secondary-lensing correlation studies, was introduced by Munshi et al. (2011c) and was subsequently used to analyse data release from *WMAP* by Calabrese et al. (2010).

The layout of the paper is as follows. In Section 2, we briefly outline various models and parametrization of modified gravity. Next, in Section 3, we review the non-Gaussianity, at the level of bispectrum, introduced by cross-correlaion of secondaries and lensing of CMB. In Section 4, we introduce the skew-spectra associated with the MFs and compute them for various modified gravity scenarios. Section 5 is devoted to likelihood analysis using MFs. In Section 6, we discuss our results. Finally, Section 7 is reserved for concluding remarks as well as discussing the future prospects.

2 MODIFIED GRAVITY MODELS

Studies of modified gravity models can, in principle, be classified into two different frameworks (Bertschinger & Zukin 2008). The first is a model-dependent method. One can start from a specific Lagrangian, investigating its dynamical behaviour to finally give its predictions. Various viable modified gravity models have been proposed which fall into this category (Clifton et al. 2012). In this paper, we mainly focus on $f(R)$ models (see e.g. De Felice & Tsujikawa 2010, for a review), such as the Starobinsky (1980) model or the Hu–Sawicki model (Hu & Sawicki 2007a).

The other method is inspired by the parametrized post-Newtonian approach to Solar system tests of gravity. In this case, one aims to build a model-independent framework, in which many modified gravity models can be parametrized in a unified way. The simplest idea is directly to generalize the Eddington parameter ($\gamma \equiv \Phi/\Psi$; Eddington 1922) to an unknown function of space and time $\gamma(t, \boldsymbol{x})$ in a Friedmann Universe. Many studies, such as Bertschinger & Zukin (2008), Zhao et al. (2009a,b), Hojjati, Pogosian & Zhao (2011) and Giannantonio et al. (2010), show that this works quite well for large-scale structure data. This is because these parametrizations are mainly suitable for the quasi-static regime where the time evolution of the gravitational potentials are negligible compared with spatial gradients. Furthermore, if we focus on the linear analysis in the Fourier domain, then the dynamical equations can be reduced to simple algebraic relations. These allow us to perform some analytic calculations, which make the parametrization technically efficient. However, if we want to go further, beyond the quasi-static scale, even though still in the linear regime, the parametrization of modified gravity is more non-trivial. This is because at the larger scales, especially the super- or near-horizon scales, the time evolution of gravitational potentials is no longer negligible and we need to solve temporal ordinary differential equations.

Besides the above explicit parametrizations, some quite generic frameworks have been proposed, such as the Hu–Sawicki PPF formalism (Hu & Sawicki 2007b; Fang et al. 2008; Hu 2008) and its calibration version (Lombriser et al. 2013). The Hu–Sawicki PPF parametrization is defined by three functions: $g(\ln a, k_H), f_\zeta(\ln a), f_G(\ln a)$ and a single parameter c_Γ. They correspond to the metric ratio, the super-horizon relationship between the metric and density, the deviation of Newton's constant on super-horizon scale from that on quasi-static scales, and the relationship between the transition scale and the Hubble scale (Hu & Sawicki 2007b). Of course, this formalism is quite generic. However, in order to obtain the explicit parametrization form of these arbitrary functions, one needs to solve the exact equation of motion obtained from the original Lagrangian of the modified gravity theory and fit the above three functions with the exact solution. Up to now, only a few models, such as $f(R)$ and Dvali–Gabadadze–Porrati models, have been successfully implemented in the Hu–Sawicki PPF formalism. Even though, this formalism still has a great advantage for numerical purposes, since it provides a unified form to write down all the modified equations. Besides that mentioned above, there exist many other parametrizations (Linder 2005; Amendola, Kunz & Sapone 2008; Bean & Tangmatitham 2010; Baker et al. 2011, 2013; Bertacca, Bartolo & Matarrese 2011; Bloomfield et al. 2012; Branx et al. 2012; Gubitosi et al. 2013).

2.1 Hu–Sawicki $f(R)$ model

As an example of a model-dependent method, the Lagrangian of Hu–Sawicki model (hereafter HS) reads

$$f(R) = -m^2 \frac{c_1 (R/m^2)^n}{c_2 (R/m^2)^n + 1}\,; \qquad m^2 \equiv H_0^2 \Omega_{\rm m} = (8315\,{\rm Mpc})^{-2} \left(\frac{\Omega_{\rm m} h^2}{0.13}\right). \tag{1}$$

As shown by Hu & Sawicki (2007a), this model can pass the local Solar system tests. The non-linear terms in $f(R)$ introduce fourth-order derivatives into this theory, rather than the more familiar second-order derivatives. Fortunately, we can reduce the derivatives to second order by defining an extra scalar field $\chi \equiv ({\rm d}f/{\rm d}R)$, namely the 'scalaron', which absorbs the higher derivatives. The *Compton wavelength* of the scalaron is defined as

$$B = \frac{f_{RR}}{1 + f_R} R' \frac{H}{H'}\,, \tag{2}$$

with $f_R = {\rm d}f/{\rm d}R$, $f_{\rm RR} = {\rm d}^2 f/{\rm d}R^2$ and $' \equiv {\rm d}/{\rm d}\ln a$. In the high-curvature regime, equation (1) can be expanded w.r.t. (m^2/R) as

$$\lim_{(m^2/R)\to 0} f(R) \approx -\frac{c_1}{c_2} m^2 + \frac{c_1}{c_2^2} m^2 \left(\frac{m^2}{R}\right)^n + \cdots . \tag{3}$$

From equation (3), we can see that the first and second terms represent a cosmological term and a deviation from it, respectively. In order to mimic Λ cold dark matter (ΛCDM) evolution on the background, the value of (c_1/c_2) can be fixed (Hu & Sawicki 2007a) such that $(c_1/c_2) = 6(\Omega_\Lambda/\Omega_{\rm m})$. By using this relation the number of free parameters can be reduced to two. From the above analysis, we can see that, strictly speaking, due to the appearances of correction terms to the cosmological constant, the HS model cannot exactly mimic ΛCDM. Since (m^2/R) increases very fast with time, the largest value (at the present epoch) is $(m^2/R) \sim 0.03$, the largest deviation to the ΛCDM background happens when $n = 1$, with 1 per cent errors, corresponding to $(m^2/R)c_2 \sim 0.01$ in equation (3). For larger n values, such as $n = 4, 6$, we can safely neglect this theoretical error. As shown by Hu et al. (2013a), for $n = 1$, this 1 per cent deviation from ΛCDM brings a 10 per cent error in the variance of the parameter B_0, while for $n = 4$, 6, our results are not affected.

Without loss of generality, we can choose the two free parameters to be (n, c_2). However, for more general $f(R)$ models, the ΛCDM evolution of the background can be reproduced exactly by only introducing one free parameter (Song et al. 2007a). This means that there exists some degeneracy between the two parameters. Usually General Relativity (GR) is recovered when $B_0 = 0$. As demonstrated by Hu et al. (2013a), no matter what value n takes, we are always allowed to set $B_0 = 0$ by adjusting c_2. Furthermore, in order to mimic ΛCDM on the background, c_2 and n need to satisfy one constraint: the first term in the denominator of equation (1) should be much larger than the second. This condition gives

$$B_0^{\rm max} = \begin{cases} 0.1, & (n = 1)\,, \\ 1.2, & (n = 4)\,, \\ 4.0, & (n = 6)\,. \end{cases} \tag{4}$$

Hu et al. (2013a) forecast that *Planck*[1] is expected to reduce the error bars on the modified gravity parameter B_0 by at least one order of magnitude compared to *WMAP*. The spectrum–bispectrum joint analysis can further improve the results by a factor ranging from 1.14 to 5.32 depending on the value of n.

2.2 Hu–Sawicki PPF formalism

In contrast to the above subsection, in what follows, we will consider all possibilities in $f(R)$ gravity which can mimic the ΛCDM background in the Hu–Sawicki PPF formalism (hereafter PPF). The logic of the PPF formalism is the following: first, considering two limits in the linear fluctuation regimes, the super-horizon and quasi-static regimes. In the former, the time derivatives are much more important than the spatial derivatives and in the latter limit the vice versa; then, derive and solve the gravitational equations in these limits. Given the knowledge of these two limits, one can propose two modified gravitational equations which recover the above results in the super-horizon and quasi-static limits, respectively. Finally, we integrate all the linear scales using the proposed equations.

For the metric scalar fluctuations, in principle, we have only two degrees of freedom, such as Φ (Newtonian potential) and Ψ (curvature potential) in the conformal Newtonian gauge, which means we only need two dynamical equations. For PPF, these two master equations are the modified Poisson equation and the equation for Γ:

$$k^2[\Phi_- + \Gamma] = 4\pi G a^2 \rho_{\rm m} \Delta_{\rm m}\,; \qquad \Phi_- = \Phi - \Psi \tag{5}$$

$$\left(1 + c_\Gamma^2 k_H^2\right)[\Gamma' + \Gamma + c_\Gamma^2 k_H^2(\Gamma - f_G \Phi_-)] = S, \tag{6}$$

where the source term S is given by

$$S = -\left[\frac{1}{g+1}\frac{H'}{H} + \frac{3}{2}\frac{H_{\rm m}^2}{H^2 a^3}(1 + f_\zeta)\right]\frac{V_{\rm m}}{k_H} + \left[\frac{g' - 2g}{g+1}\right]\Phi_-\,. \tag{7}$$

$V_{\rm m}$ here is the scalar velocity fluctuation of the matter in both the comoving and Newtonian gauge and $H_{\rm m}$ is the contribution to Hubble parameter from the matter component; see Hu & Sawicki (2007b) for more details.

In equation (6), the coefficient c_Γ represents the relationship between the transition scale and the Hubble scale, and the function f_ζ gives the relationship between the metric and the density perturbation. For $f(R)$ models, we have $c_\Gamma = 1, f_\zeta = c_\zeta g$ and the function $g(\ln a, k)$ can be expressed as follows.

$$g(\ln a, k) = \frac{g_{\rm SH} + g_{\rm QS}(c_g k_H)^{n_g}}{1 + (c_g k_H)^{n_g}}\,, \qquad g_{\rm QS} = -1/3\,, \quad n_g = 2\,, \quad c_g = 0.71\sqrt{B(t)}\,. \tag{8}$$

The above descriptions have been implemented in the publicy available PPF module (Fang et al. 2008) of CAMB[2] (Lewis, Challinor & Lasenby 2000). The current constraints on general $f(R)$ models within the PPF are $B_0 < 0.42$ (95 per cent CL) by using CMB and ISW–galaxy

[1] http://sci.esa.int/science-e/www/area/index.cfm?fareaid=17
[2] http://camb.info/

correlation data, and a strong constraint $B_0 < 1.1 \times 10^{-3}$ at 95 per cent CL (Lombriser et al. 2012). using a larger set of data, such as *WMAP*5,[3] ACBAR,[4] CBI,[5] VSA, Union,[6] SHOES and BAO data.

2.3 Bertschinger–Zukin formalism

Another popular phenomenological parametrization was proposed by Bertschinger & Zukin (2008, hereafter BZ) and implemented in the Einstein–Boltzmann solver MGCAMB[7] (Zhao et al. 2009a; Hojjati et al. 2011). The logic of this parametrization is to re-write the two gravitational potentials in terms of two observation-related variables, the time- and scale-dependent Newton constant $G\mu(a, k)$ and the so-called gravitational slip $\gamma(a, k)$:

$$k^2\Psi = -4\pi G a^2 \mu(a,k)\rho\Delta; \qquad \frac{\Phi}{\Psi} = \gamma(a,k). \tag{9}$$

G is the Newton constant in the laboratory. Furthermore, in the quasi-static regime, Bertschinger and Zukin propose a quite efficient parametrizations for these two quantities (see also Zhao et al. 2009a):

$$\mu(a,k) = \frac{1+\frac{4}{3}\lambda_1^2k^2a^4}{1+\lambda_1^2k^2a^4}; \qquad \gamma(a,k) = \frac{1+\frac{2}{3}\lambda_1^2k^2a^4}{1+\frac{4}{3}\lambda_1^2k^2a^4}. \tag{10}$$

The above parametrization was refined to take the ISW effect into account through an empirical formula (Giannantonio et al. 2010)

$$\mu(a,k) = \frac{1}{1-1.4\times10^{-8}|\lambda_1|^2a^3}\left[\frac{1+\frac{4}{3}\lambda_1^2k^2a^4}{1+\lambda_1^2k^2a^4}\right]. \tag{11}$$

Compared with PPF, one can easily see the physical meaning of parameter λ_1, as the present Compton wavelength $\lambda_1^2 = B_0c^2/(2H_0^2)$. Besides that, we can also see that BZ is much more efficient than the former, because in BZ one only needs to solve an algebraic relation, equation (9) or equivalently equation (11), while in PPF, we have to integrate differential equations, equations (5) and (6). The price BZ pays is that it might not account for the ISW effect properly in the super-horizon regime. However, recently it was shown (Hojjati et al. 2012b) that for all practical purposes BZ for $f(R)$ model with small B_0 is good enough even if one considers the near-horizon scale: the maximum error is $\mathcal{O}$(2 per cent). Recently, it was shown by (Hu et al. 2013a) that the temperature and lensing power-spectrum data from *Planck* alone can give an upper bound on $B_0 < 0.91$ at 95 per cent CL.

3 ISW-LENSING CROSS-SPECTRA AS A PROBE OF MODIFIED GRAVITY THEORIES

We will be dealing with the secondary bispectra involving the lensing of both primary anisotropies and other secondaries. Following Spergel & Goldberg (1999), Goldberg & Spergel (1999) and Cooray & Hu (2000), we start by expanding the observed temperature anisotropy $\Theta(\hat\Omega) = \delta T(\hat\Omega)/T$ in terms of the primary contribution $\Theta_{\rm P}(\hat\Omega)$, the secondary contribution $\Theta_{\rm S}(\hat\Omega)$ and lensing of the primary $\Theta_{\rm L}(\hat\Omega)$:

$$\Theta(\hat\Omega) = \Theta_{\rm P}(\hat\Omega) + \Theta_{\rm L}(\hat\Omega) + \Theta_{\rm S}(\hat\Omega) + \cdots. \tag{12}$$

Here, $\hat\Omega = (\theta, \phi)$ is the angular position on the surface of the sky. Expanding the respective contributions in terms of spherical harmonics $Y_{lm}(\hat\Omega)$ we can write

$$\Theta_{\rm P}(\hat\Omega) \equiv \sum_{\ell m}(\Theta_{\rm p})_{\ell m}Y_{\ell m}(\hat\Omega); \quad \Theta_{\rm L}(\hat\Omega) \equiv \sum_{\ell m}[\nabla\psi(\hat\Omega)\cdot\nabla\Theta_{\rm P}(\hat\Omega)]_{\ell m}\,Y_{\ell m}(\hat\Omega); \quad \Theta_{\rm S}(\hat\Omega) \equiv \sum_{\ell m}(\Theta_{\rm S})_{\ell m}Y_{\ell m}(\hat\Omega). \tag{13}$$

Here, $\psi(\hat\Omega)$ is the projected lensing potential (Goldberg & Spergel 1999; Spergel & Goldberg 1999). The secondary bispectrum for the CMB takes contributions from products of P, L and S terms with varying order. The bispectrum $B^{\rm PLS}_{\ell_1\ell_2\ell_3}$ is defined as follows (see Bartolo et al. 2004 for generic discussion of the bispectrum and its symmetry properties).

$$\begin{aligned} B^{\rm PLS}_{\ell_1\ell_2\ell_3} &\equiv \sum_{m_1m_2m_3}\begin{pmatrix}\ell_1 & \ell_2 & \ell_3\\ m_1 & m_2 & m_3\end{pmatrix}\int\left\langle\Theta_{\rm P}(\hat\Omega_1)\Theta_{\rm L}(\hat\Omega_2)\Theta_{\rm S}(\hat\Omega_3)\right\rangle Y^*_{\ell_1m_1}(\hat\Omega_1)Y^*_{\ell_2m_2}(\hat\Omega_2)Y^*_{\ell_3m_3}(\hat\Omega_3){\rm d}\hat\Omega_1\,{\rm d}\hat\Omega_2\,{\rm d}\hat\Omega_3;\\ &\equiv \sum_{m_1m_2m_3}\begin{pmatrix}\ell_1 & \ell_2 & \ell_3\\ m_1 & m_2 & m_3\end{pmatrix}\langle(\Theta_{\rm P})_{\ell_1m_1}(\Theta_{\rm L})_{\ell_2m_2}(\Theta_{\rm S})_{\ell_3m_3}\rangle. \end{aligned} \tag{14}$$

[3] http://map.gsfc.nasa.gov/
[4] http://cosmology.berkeley.edu/group/swlh/acbar/
[5] http://www.astro.caltech.edu/~tjp/CBI/
[6] http://supernova.lbl.gov/Union/
[7] http://www.sfu.ca/~aha25/MGCAMB.html

The angular brackets represent *ensemble* averages. The matrices denote 3*J* symbols (Edmonds 1968) and the asterisks denote complex conjugation. It is possible to invert the relation assuming isotropy of the background Universe:

$$\langle(\Theta_{\rm P})_{\ell_1 m_1}(\Theta_{\rm L})_{\ell_2 m_2}(\Theta_{\rm S})_{l_3 m_3}\rangle = \begin{pmatrix} \ell_1 & \ell_2 & \ell_3 \\ m_1 & m_2 & m_3 \end{pmatrix} B^{\rm PLS}_{\ell_1\ell_2\ell_3}. \tag{15}$$

Finally, the bispectrum $B^{\rm PLS}_{\ell_1\ell_2\ell_3}$ is expressed in terms of the unlensed primary power spectrum $\mathcal{C}_\ell^{\rm TT} = \langle(\Theta_{\rm P})_{lm}(\Theta^*_{\rm P})_{\ell m}\rangle$ and the cross-spectra $\mathcal{C}_\ell^{\phi{\rm T}}$ (to be defined below) as follows.

$$B^{\rm PLS}_{\ell_1\ell_2\ell_3} \equiv b^{\rm ISW\text{-}len}_{\ell_1\ell_2\ell_3} I_{\ell_1\ell_2\ell_3}; \tag{16}$$

$$b^{\rm ISW-lens}_{\ell_1\ell_2\ell_3} = -\frac{1}{2}\left[\mathcal{C}^{\phi{\rm T}}_{\ell_3}\mathcal{C}^{\rm TT}_{\ell_1}(\Pi_{\ell_2} - \Pi_{\ell_1} - \Pi_{\ell_3}) + {\rm cyc.perm.}\right]; \tag{17}$$

$$I_{\ell_1\ell_2\ell_3} \equiv \sqrt{\frac{\Xi_{\ell_1}\Xi_{\ell_2}\Xi_{\ell_3}}{4\pi}} \begin{pmatrix} \ell_1 & \ell_2 & \ell_3 \\ 0 & 0 & 0 \end{pmatrix}; \tag{18}$$

$$\Pi_\ell = \ell(\ell+1); \quad \Xi_\ell = (2\ell+1). \tag{19}$$

See Spergel & Goldberg (1999) and Goldberg & Spergel (1999) for a derivation. The long-wavelength modes of ISW couple with the short-wavelength modes of fluctuations generated due to lensing, hence, the non-zero cross-spectrum $\mathcal{C}_\ell^{\phi{\rm T}}$. The reduced bispectrum above is denoted as $b^{\rm ISW\text{-}lens}_{\ell_1\ell_2\ell_3}$. To simplify the notation for the rest of this paper, we henceforth drop the superscript PLS from the bispectrum $B_{\ell_1\ell_2\ell_3}$. The cross-spectrum $\mathcal{C}_\ell^{\phi{\rm T}}$ introduced above represents the cross-correlation between the projected lensing potential $\psi(\hat\Omega)$ and the secondary contribution $\Theta_{\rm S}(\hat\Omega)$:

$$\langle\psi(\hat\Omega)\Theta_{\rm S}(\hat\Omega')\rangle = \frac{1}{4\pi}\sum_{\ell=2}^{\ell_{\rm max}} \Xi_\ell\, \mathcal{C}_\ell^{\phi{\rm T}} P_\ell(\hat\Omega\cdot\hat\Omega'), \tag{20}$$

where P_ℓ are Legendre polynomials. The cross-spectrum $\mathcal{C}_\ell^{\phi{\rm T}}$ takes different forms for ISW-lensing, Rees–Sciama (RS)-lensing or SZ-lensing correlations and we assume zero primordial non-Gaussianity. The reduced bispectrum $b_{\ell_1\ell_2\ell_3}$ defined above using the notation $I_{\ell_1\ell_2\ell_3}$ is useful in separating the angular dependence from the dependence on the power spectra $\mathcal{C}_\ell^{\phi{\rm T}}$ and $\mathcal{C}_\ell^{\phi{\rm T}}$. We will use this to express the topological properties of the CMB maps. The $\mathcal{C}_\ell^{\phi{\rm T}}$ parameters for lensing secondary correlations are displayed in Fig. 2.

The beam $b_\ell(\theta_{\rm b})$ and the noise of a specific experiment are characterized by the parameters $\sigma_{\rm beam}$ and $\sigma_{\rm rms}$ as

$$b_\ell(\theta_{\rm b}) = \exp[-\Pi\sigma^2_{\rm beam}];\ \ \sigma_{\rm beam} = \frac{\theta_{\rm b}}{\sqrt{8\ln(2)}};\ \ n_\ell = \sigma^2_{\rm rms}\Omega_{\rm pix};\quad \Omega_{\rm pix} = \frac{4\pi}{N_{\rm pix}}, \tag{21}$$

where $\sigma_{\rm rms}$ is the rms noise per pixel, which depends on the full width at half-maximum or FWHM of the beam, $\theta_{\rm b}$. The number of pixels $N_{\rm pix}$ required to cover the sky determines the size of the pixels $\Omega_{\rm pix}$. To incorporate the effect of experimental noise and the beam, we replace $\mathcal{C}_\ell \to \mathcal{C}_\ell b^2_\ell(\theta_{\rm b}) + n_\ell$, and the normalization of the skew-spectra that we will introduce later will be affected by the experimental beam and noise. The computation of the scatter will also depend on these parameters.

The reduced bispectrum for the unresolved PS can be characterized by a constant amplitude $b_{\rm PS}$, i.e. the angular-averaged bispectrum $B^{\rm PS}_{\ell_1\ell_2\ell_3}$ for PS is given by $B^{\rm PS}_{\ell_1\ell_2\ell_3} = b_{\rm PS} I_{\ell_1\ell_2\ell_3}$; for our numerical results, we will take $b_{\rm PS} = 10^{-29}$.

The optimal estimators for lensing-secondary mode-coupling bispectrum have been recently discussed by Munshi et al. (2011c). The estimators that we propose here are relevant in the context of constructing the MFs.

3.1 Computation of $\mathcal{C}_\ell^{\rm TT}$, $\mathcal{C}_\ell^{\phi{\rm T}}$ and $\mathcal{C}_\ell^{\phi\phi}$

The ISW effect and lensing potential ϕ can both be expressed in terms of the Weyl potential $\Phi - \Psi$ as

$$\left.\frac{\delta T(\hat\Omega)}{T}\right|_{\rm ISW} = \int {\rm d}r \frac{\rm d}{{\rm d}\tau}(\Phi - \Psi); \quad \phi(\hat\Omega) = -\int_0^{r_s} {\rm d}r \frac{r_s - r}{r r_s}(\Phi - \Psi). \tag{22}$$

Assuming a flat Universe, we can express the cross-spectra $C_\ell^{\phi{\rm T}}$, the ISW contribution $C_\ell^{\rm TT}$ to the power spectrum and the lensing potential spectrum $C_\ell^{\phi\phi}$ as follows (Hu 2000)

$$C_\ell^{\phi{\rm T}} = \frac{2\pi^2}{\ell^3}\int_0^{r_s} {\rm d}r\, r\, W^{\rm ISW}(r) W^{\rm Len}(r)\Delta^2_\Phi(k,0)\Big|_{k=\ell\frac{H_0}{r}}; \tag{23}$$

$$C_\ell^{\rm TT} = \frac{2\pi^2}{\ell^3}\int_0^{r_s} {\rm d}r\, r\, W^{\rm ISW}(r) W^{\rm ISW}(r)\Delta^2_\Phi(k,0)\Big|_{k=\ell\frac{H_0}{r}}; \tag{24}$$

$$C_\ell^{\phi\phi} = \frac{2\pi^2}{\ell^3}\int_0^{r_s} \mathrm{d}r\, r\, W^{\rm Len}(r) W^{\rm Len}(r) \Delta^2_\Phi(k,0)\Big|_{k=\ell\frac{H_0}{r}}, \tag{25}$$

where r_s is the comoving distance and $r(z) = \int_0^z [H_0/H(z')]\mathrm{d}z'$. We can express the gravitational potential power spectrum $\Delta^2_\Phi(k,z)$ by using the transfer function $T(k)$ and the growth factor $[f(z)/(1+z)]$:

$$\Delta^2_\Phi(k,z) = \frac{9}{4}\Omega_{\rm m}^2 \delta_H^2 F(z) T^2(k) \left(\frac{k}{H_0}\right)^{n-1}; \tag{26}$$

with δ_H denoting the amplitude of matter density fluctuation at the present Hubble scale. The window functions $W^{\rm ISW}(r)$ and $W^{\rm Len}(r)$ used above in equations (23)–(25) are expressed as follows.

$$W^{\rm ISW}(r) = -\frac{\mathrm{d}}{\mathrm{d}r}[(1+\gamma)F], \qquad W^{\rm Len}(r) = -(1+\gamma)F(r)\frac{(r_s - r)}{r\, r_s}. \tag{27}$$

This is the expression used in equation (19) to construct the bispectrum which was used to compute the optimized skew-spectra of equation (35) and the sub-optimal versions in equations (29)–(31) to be introduced in Section 4 later.

4 MFs AND ASSOCIATED POWER SPECTRA

The study of non-Gaussianity is usually primarily focused on the bispectrum, as this saturates the Cramér–Rao bound (Babich 2005; Kamionkowski, Smith & Heavens 2011) and is therefore in a sense optimal. However, in practice, it is difficult to probe the entire configuration dependence using noisy data (Munshi & Heavens 2010). An alternative is to use cumulant correlators, which are multipoint correlators collapsed to encode two-point statistics. These were introduced into galaxy clustering by Szapudi & Szalay (1999), and were later found to be useful for analysing projected surveys such as the APM galaxy survey (Munshi, Melott & Coles 2000). Being two-point statistics, they can be analysed in multipole space by defining an associated power spectrum (Cooray 2001). Recent studies by Cooray, Li & Melchiorri (2008) have demonstrated their wider applicability including, e.g. in 21 cm studies. In more recent studies, the skew- and kurt-spectra were found to be useful for analysing temperature (Munshi & Heavens 2010) as well as polarization maps (Munshi et al. 2011a) and maps of secondaries from CMB experiments (Munshi et al. 2012a; Munshi, Coles & Heavens 2013a) and in weak lensing studies (Munshi et al. 2012b). The MFs are well-known morphological descriptors which are used in the study of random fields. Morphological properties are the properties that remain invariant under rotation and translation (see Hadwiger 1959 for a more formal introduction). They are defined over an excursion set Σ for a given threshold ν. The three MFs that are defined for 2D studies can be expressed as (Pratten & Munshi 2012)

$$V_0(\nu) = \int_\Sigma \mathrm{d}a; \quad V_1(\nu) = \frac{1}{4}\int_{\partial\Sigma} \mathrm{d}l; \quad V_2(\nu) = \frac{1}{2\pi}\int_{\partial\Sigma} \kappa \mathrm{d}l. \tag{28}$$

Here $\mathrm{d}a$, $\mathrm{d}l$ are the elements for the excursion set Σ and its boundary $\partial\Sigma$. The MFs $V_k(\nu)$ correspond, respectively, to the area of the excursion set Σ, the length of its boundary $\partial\Sigma$ and the integral curvature along its boundary (which is also related to the genus g and hence the Euler characteristics χ).

Following earlier studies (Munshi et al. 2012b, 2013a,b), we introduce three different skew-spectra associated with MFs for an arbitrary cosmological projected field Ψ:

$$S_\ell^{(0)} \equiv \frac{1}{N_0} S_\ell^{(\Psi^2,\Psi)} \equiv \frac{1}{N_0}\frac{1}{\Xi_\ell}\sum_m \mathrm{Real}([\Psi]_{\ell m}[\Psi^2]^*_{\ell m}) = \frac{1}{N_0}\sum_{\ell_1\ell_2} B_{\ell\ell_1 l_2} J_{\ell\ell_1\ell_2}; \tag{29}$$

$$S_\ell^{(1)} \equiv \frac{1}{N_1} S_\ell^{(\Psi^2,\nabla\Psi)} \equiv \frac{1}{N_1}\frac{1}{\Xi_\ell}\sum_m \mathrm{Real}([\nabla^2\Psi]_{\ell m}[\Psi^2]^*_{\ell m}) = \frac{1}{N_1}\sum_{\ell_1\ell_2}[\Pi_\ell + \Pi_{\ell_1} + \Pi_{\ell_2}] B_{\ell\ell_1\ell_2} J_{\ell\ell_1\ell_2}; \tag{30}$$

$$\begin{aligned} S_\ell^{(2)} &\equiv \frac{1}{N_2} S_\ell^{(\nabla\Psi\cdot\nabla\Psi,\nabla^2\Psi)} \equiv \frac{1}{N_2}\frac{1}{\Xi_\ell}\sum_m \mathrm{Real}([\nabla\Psi\cdot\nabla\Psi]_{\ell m}[\nabla^2\Psi]^*_{lm}) \\ &= \frac{1}{N_2}\sum_{\ell_1\ell_2}\frac{1}{2}[[\Pi_\ell + \Pi_{\ell_1} - \Pi_{\ell_2}]\Pi_{\ell_2} + \mathrm{cyc.perm.}] B_{\ell\ell_1\ell_2} J_{\ell\ell_1\ell_2}; \end{aligned} \tag{31}$$

$$J_{\ell_1\ell_2\ell_3} \equiv \frac{I_{\ell_1\ell_2\ell_3}}{\Xi_{\ell_1}} = \sqrt{\frac{\Sigma_{\ell_2}\Sigma_{\ell_3}}{\Sigma_{\ell_1} 4\pi}} \begin{pmatrix} \ell_1 & \ell_2 & \ell_3 \\ 0 & 0 & 0 \end{pmatrix}; \tag{32}$$

$$S^{(i)} = \sum_\ell \Xi_\ell S_\ell^{(i)}; \tag{33}$$

$$N_0 = 12\pi\sigma_0^4; \quad N_1 = 16\pi\sigma_0^2\sigma_1^2; \quad N_2 = 8\pi\sigma_1^4. \tag{34}$$

In contrast to these MF-based quantities, the optimized skew-spectra $S_\ell^{\rm opt}$ for two different types of non-Gaussianity is defined by the following expression:

$$S_\ell^{\rm opt}(X,Y) = \frac{1}{6}\sum_{\ell_1\ell_2}\frac{B^X_{\ell\ell_1\ell_2}B^Y_{\ell\ell_1\ell_2}}{\mathcal{C}_\ell^{\rm tot}\mathcal{C}_{\ell_1}^{\rm tot}\mathcal{C}_{\ell_2}^{\rm tot}}; \qquad S^{\rm opt}(X,Y) = \sum_\ell S_\ell^{\rm opt}(X,Y). \tag{35}$$

The three skew-spectra associated with MFs, defined in equations (29)–(31), for various theories of modified gravity are shown in Fig. 4 as a function of harmonic ℓ for PPF, BZ and HS models. Clearly, the one-point estimator defined in equation (34) will have nearly vanishing amplitude due to cancellation originating from the oscillatory pattern seen in all three skew-spectra associated with MFs. The FWHM is fixed at $\theta_{\rm b} = 5'$. The noise level is chosen to match the *Planck* 143 GHz channel. It is interesting to note that the extrema of $\ell^3 S_\ell^{(0)}$ for all models occurs roughly at similar ℓ values. We display four different values of B_0 for each models $B_0 = 10^{-3}$ (solid), 10^{-2} (short dashed), 10^{-1} (long dashed) and 1 (dot–dashed), respectively. For HS models, we choose two different values for B_0, i.e. $B_0 = 10^{-3}$ and 10^{-2}. In agreement with what we found for optimized estimators, the skew-spectra for the HS models with low n values show a greater degree of sensitivity to B_0 compared to their high-n counterparts, which roughly mimic their PPF or BZ counterparts.

5 LIKELIHOOD ANALYSIS USING SKEW-SPECTRA

In this section, we construct the joint covariance matrices for skew-spectra and ordinary spectra and provide results of a likelihood analysis forecast for the parameter B_0.

The Gaussian contributions to the covariance matrix can be expressed in terms of the total power spectrum $\mathcal{C}_\ell^{\rm tot}$ alone, which in terms of beam b_ℓ and the noise power spectrum n_ℓ takes the form $\mathcal{C}_\ell^{\rm tot} = \mathcal{C}_\ell^{\rm TT} b_\ell^2 + n_\ell$:

$$\begin{aligned}\mathcal{S}^{(ij)}_{\ell\ell'} &= \langle \delta S_\ell^{(i)} \delta S_{\ell'}^{(j)}\rangle = \langle S_\ell^{(i)} S_{\ell'}^{(j)}\rangle - \langle S_\ell^{(i)}\rangle\langle S_{\ell'}^{(j)}\rangle \\ &= \frac{1}{N_{(i)}}\frac{1}{N_{(j)}}\mathcal{C}_\ell^{\rm tot}\sum_{\ell_1\ell_2}\mathcal{C}_{\ell_1}^{\rm tot}\mathcal{C}_{\ell_2}^{\rm tot} J^{(i)}_{\ell\ell_1\ell_2}\left[\left(J^{(j)}_{\ell'\ell_1\ell_2} + J^{(j)}_{\ell'\ell_2\ell} + J^{(j)}_{\ell'\ell\ell_1}\right) + (-1)^{\ell+\ell_1+\ell_2}\left(J^{(j)}_{\ell'\ell_2\ell_1} + J^{(j)}_{\ell'\ell\ell_2} + J^{(j)}_{\ell'\ell_1\ell}\right)\right];\end{aligned} \tag{36}$$

$$J^{(0)}_{\ell_1\ell_2\ell_3} = J_{\ell_1\ell_2\ell_3}; \quad J^{(1)}_{\ell_1\ell_2\ell_3} = \left(\Pi_{\ell_1} + \Pi_{\ell_2} + \Pi_{\ell_3}\right) J_{\ell_1\ell_2\ell_3}; \quad J^{(2)}_{\ell_1\ell_2\ell_3} = \left((\Pi_{\ell_1} + \Pi_{\ell_2} - \Pi_{\ell_3})\Pi_{\ell_3} + \text{cyc.perm.}\right) J_{\ell_1\ell_2\ell_3}. \tag{37}$$

We use the following expression in our derivation (Bartolo et al. 2004):

$$\langle B_{\ell_1\ell_2\ell_3} B_{\ell'_1\ell'_2\ell'_3}\rangle = \mathcal{C}_{\ell_1}^{\rm tot}\mathcal{C}_{\ell_2}^{\rm tot}\mathcal{C}_{\ell_3}^{\rm tot}\left[\left(\delta^{\ell'_1\ell'_2\ell'_3}_{\ell_1\ell_2\ell_3} + \delta^{\ell'_3\ell'_1\ell'_2}_{\ell_1\ell_2\ell_3} + \delta^{\ell'_2\ell'_3\ell'_1}_{\ell_1\ell_2\ell_3} + (-1)^{\ell_1+\ell_2+\ell_3}\left(\delta^{\ell'_1\ell'_3\ell'_2}_{\ell_1\ell_2\ell_3} + \delta^{\ell'_2\ell'_1\ell'_3}_{\ell_1\ell_2\ell_3} + \delta^{\ell'_3\ell'_2\ell'_1}_{\ell_1\ell_2\ell_3}\right)\right];$$

$$\delta^{\ell'_1\ell'_2\ell'_3}_{\ell_1\ell_2\ell_3} = \delta_{\ell_1\ell'_1}\delta_{\ell_2\ell'_2}\delta_{\ell_3\ell'_3}. \tag{38}$$

Note that the $3J$ symbols involved in the definitions of $S_\ell^{(i)}$ all have the azimuthal quantum numbers $m_i = 0$ in which case we have non-zero $3J$ symbols only when $(\ell + \ell_1 + \ell_2) =$ even, thus, $(-1)^{\ell+\ell_1+\ell_2} = 1$. Thus, we notice that $J^{(i)}_{\ell\ell_1\ell_2}$ is symmetric under the exchange of the last two indices, i.e. ℓ_1 and ℓ_2. Using these facts, after a straightforward but tedious calculation, we can further simplify equation (36) to

$$\mathbb{S}^{(ij)}_{\ell\ell'} \equiv \mathcal{S}^{(ij)}_{\ell\ell'} = \langle \delta S_\ell^{(i)} \delta S_{\ell'}^{(j)}\rangle = \frac{1}{N_{(i)}}\frac{1}{N_{(j)}}\left[2\,\delta_{\ell\ell'}\,\mathcal{C}_\ell^{\rm tot}\sum_{\ell_1\ell_2}\mathcal{C}_{\ell_1}^{\rm tot}\mathcal{C}_{\ell_2}^{\rm tot} J^{(i)}_{\ell\ell_1\ell_2} J^{(j)}_{\ell\ell_1\ell_2} + 4\,\mathcal{C}_\ell^{\rm tot}\mathcal{C}_{\ell'}^{\rm tot}\sum_{\ell_1}\mathcal{C}_{\ell_1}\, J^{(i)}_{\ell\ell'\ell_1} J^{(j)}_{\ell'\ell\ell_1}\right]. \tag{39}$$

The first term contributes only to diagonal entries of the covariance matrix while the second term contributes also to the off-diagonal terms. This is the expression we have used in our numerical computations. The covariance matrix involving the bispectrum derived above is generic but depends on the assumption that the non-Gaussianity is weak, i.e. $\langle B_{\ell_1\ell_2\ell_3}\rangle \simeq 0$ and can also be used for likelihood calculations of primordial non-Gaussianity using MFs (Munshi et al. 2013c).

For the one-point estimators introduced previously, $S^{(i)} = \sum_\ell \Xi_\ell S_\ell^{(i)}$, the covariance matrix $\mathcal{S}^{(ij)}$ takes the following form:

$$\mathcal{S}^{(ij)} = \langle \delta S^{(i)} \delta S^{(j)}\rangle = \sum_{\ell\ell'}\Xi_\ell\,\Xi_{\ell'}\mathcal{S}^{(ij)}_{\ell\ell'} = \frac{1}{N_{(i)}}\frac{1}{N_{(j)}}\sum_{\ell_1\geq\ell_2\geq\ell_3}\mathcal{C}_{\ell_1}^{\rm tot}\mathcal{C}_{\ell_2}^{\rm tot}\mathcal{C}_{\ell_3}^{\rm tot}\, I^{(i)}_{\ell_1\ell_2\ell_3} I^{(j)}_{\ell_1\ell_2\ell_3}. \tag{40}$$

Finally, the covariance of the optimum estimator $S_\ell^{\rm opt}$ defined in equation (35) is given by the following expression:

$$\langle \delta S_\ell^{\rm opt}\delta S_{\ell'}^{\rm opt}\rangle = \frac{1}{18}\delta_{\ell\ell'}\sum_{\ell_a\ell_b}\frac{B^2_{\ell\ell_a\ell_b}}{\mathcal{C}_\ell^{\rm tot}\mathcal{C}_{\ell_a}^{\rm tot}\mathcal{C}_{\ell_b}^{\rm tot}} + \frac{1}{9}\sum_{l_a}\frac{B^2_{\ell\ell'\ell_a}}{\mathcal{C}_\ell^{\rm tot}\mathcal{C}_{\ell'}^{\rm tot}\mathcal{C}_{\ell_a}^{\rm tot}} = \frac{1}{3}\delta_{\ell\ell'}S_\ell^{\rm opt} + \frac{1}{9}\sum_{l_a}\frac{B^2_{\ell\ell'\ell_a}}{\mathcal{C}_\ell^{\rm tot}\mathcal{C}_{\ell'}^{\rm tot}\mathcal{C}_{\ell_a}^{\rm tot}}. \tag{41}$$

$$\mathbb{S}^{\rm opt} \equiv \langle \delta S^{\rm opt}\delta S^{\rm opt}\rangle = \sum_\ell S_\ell^{\rm opt} = S^{\rm opt}. \tag{42}$$

This result agrees with the previous calculation of Munshi & Heavens (2010), using Fisher matrices in the limit of all-sky coverage. The results given there include additional correction terms (termed 'β'), related to the so-called *linear*, and *cubic* ('α') terms, due to partial-sky

coverage. The likelihoods for the MFs and the optimal skew-CLs are

$$\mathcal{L}_{\rm S} = \exp(-\chi^2_{\rm S}/2); \qquad \chi^2_{\rm S} = \sum_{ij}\sum_{\ell\ell'}\left[\delta S^{(i)}_\ell [\mathbb{S}^{(ij)}]^{-1}_{\ell\ell'}\delta S^{(i)}_{\ell'}\right]; \tag{43}$$

$$\mathcal{L}_{\rm opt} = \exp(-\chi^2_{\rm opt}/2); \qquad \chi^2_{\rm S} = \sum_{\ell\ell'}\left[\delta S^{\rm opt}_\ell [\mathbb{S}^{\rm opt}]^{-1}_{\ell\ell'}\delta S^{\rm opt}_{\ell'}\right]. \tag{44}$$

For corresponding one-point estimators, we have $\mathcal{L}_{\rm S} = \exp(-[\delta S^{\rm opt}]^2/2\mathbb{S})$ and similarly for joint analysis using all one-point MFs $\mathcal{L}_{\rm S} = \exp(-[\delta S^{(i)}][\mathbb{S}^{(ij)}]^{-1}[\delta S^{(j)}]/2)$.

Bayesian recovery of B_0: in recent works, Hikage et al. (2008a) and Ducout et al. (2013) adopted a Bayesian approach in their analysis of primordial non-Gaussianity in CMB maps using MFs. We can similarly use Bayes' theorem to write the posterior probability for B_0, $P(B_0|\boldsymbol{S})$ given the one-point MFs as the data vector $\boldsymbol{S}$:

$$P(B_0|\boldsymbol{S}) = \frac{\mathcal{L}_{\rm S}(\boldsymbol{S}|B_0)P(B_0)}{\int \mathcal{L}_{\rm S}(\boldsymbol{V}|B_0)P(B_0){\rm d}B_0}; \quad \boldsymbol{S} = (S^{(0)}, S^{(1)}, S^{(2)}). \tag{45}$$

Here, $P(B_0)$ is the prior, assumed flat. Similarly, we can also use the optimized skewness as the data vector instead of the MFs by replacing $\boldsymbol{S}$ by $S^{\rm opt}$ and the likelihood function by $\mathcal{L}_{\rm opt}(\boldsymbol{S}|B_0)$. The likelihood function in such studies is typically assumed to be Gaussian, or determined using Monte Carlo simulations. We find that the likelihood for B_0 has an extended non-Gaussian tail. Thus, the analytical covariance and the corresponding likelihood derived here will be useful in providing independent estimates and related error bars for sanity checks of results derived through Monte Carlo simulations.

6 RESULTS

We have introduced three different MFs in this study and compared their performance against the optimum estimator. The aim is to use CMB data to constrain the departure of modified gravity theories from GR as parametrized by the parameter B_0 that denotes the Compton wavelength of the scalaron at the present epoch. The underlying bispectrum that we probe is the one generated by correlation between ISW and lensing of the CMB. The bispectrum is constructed from $\mathcal{C}^{\rm TT}_\ell$ (Fig. 1) and $\mathcal{C}^{T\phi}_\ell$ (Fig. 2). The corresponding optimum spectrum is given in Fig. 3.

The set three skew-spectra associated with MFs or the first Minkowski Spectra $\ell^3 S^{(0)}_\ell$, defined in equations (29)–(31), for various theories of modified gravity are displayed in Figs 4–6 as a function of the harmonic ℓ. The top-left and top-middle panels in these figures corresponds to predictions from PPF and BZ, respectively. The General Relativistic prediction correspond to $B_0 = 0$ and is shown in the top-left panel (dot and long dashed line). The bottom panels correspond to the results from the HS model, for $n = 1, 4, 6$, respectively. It is interesting to note that the one-point estimator defined in equation (34) will have nearly vanishing amplitude due to cancellation originating from the oscillatory pattern seen in all three skew-spectra associated with MFs – which is one of the motivation for studying the associated

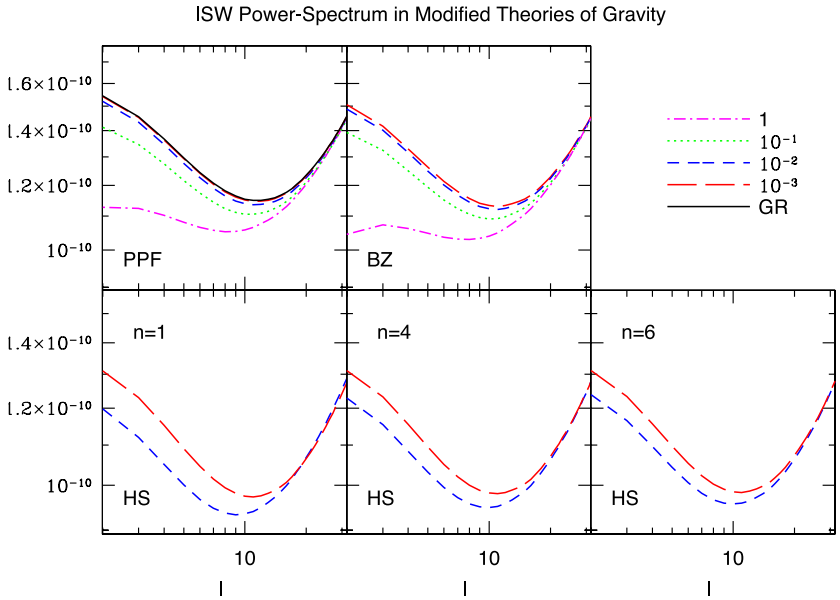

Figure 1. The ISW contribution to the (dimensionless) temperature power spectrum $\ell(\ell+1)\mathcal{C}^{\rm TT}_\ell/2\pi$ is depicted as a function of the parameter B_0 of the PPF formalism. The General Relativistic predictions correspond to $B_0 = 0$ (top-left panel). The top-left and top-right panels correspond to PPF (top-left) and BZ (top-right) formalism. For the PPF we chose $B_0 = 1, 10^{-1}, 10^{-2}, 10^{-3}$. The bottom panels correspond to the predictions from HS (Hu & Sawicki 2007a) with $n = 1$ (bottom-left), 4 (bottom-middle) and 6 (bottom-right). The values of B_0 in these plots are $B_0 = 10^{-2}$ and 10^{-3}.

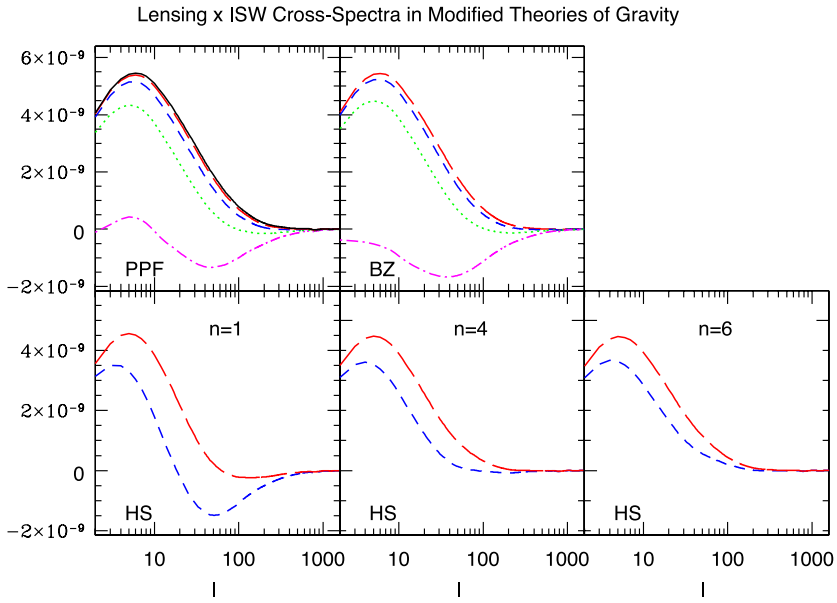

Figure 2. Same as previous plot but for the ISW-lensing cross-spectra $\ell(\ell+1)\mathcal{C}_\ell^{\phi \mathrm{T}}/2\pi$ defined in equation (20) as a function of the harmonic ℓ for various values of the parameter B_0. The line styles used for various models are same as that of Fig. 1.

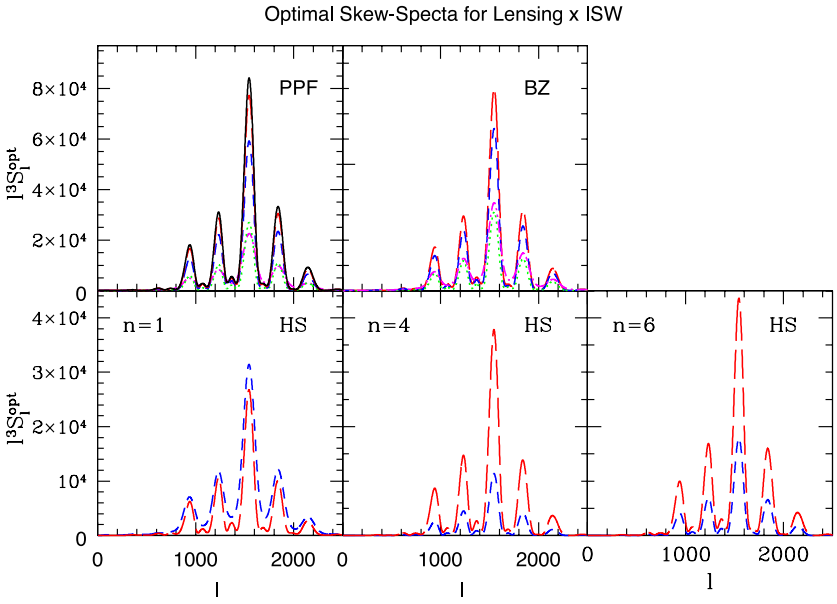

Figure 3. The optimized skew-spectra $\ell^3 S_\ell^{(\mathrm{opt})}$, introduced in equation (35), for various theories of modified gravity are displayed as a function of harmonic ℓ. The General Relativistic prediction corresponds to $B_0 = 0$. The top-left and top-middle panels correspond to the predictions from PPF and BZ, respectively. The bottom panels correspond to HS with $n = 1$ (bottom-left), 4 (bottom-middle) and 6 (bottom-right). The values of B_0 in these plots are $B_0 = 10^{-2}$ and 10^{-3}. We have used $\ell_{\mathrm{max}} = 2500$ and a Gaussian beam with FWHM $\theta_{\mathrm{b}} = 5$ arcmin for the numerical evaluation of $S_\ell^{(\mathrm{opt})}$. The line styles used for various models are same as that of Fig. 1.

power spectra. The FWHM is fixed at $\theta_{\mathrm{b}} = 5'$. The noise level is chosen to match the *Planck* 143 GHz channel. It is interesting to note that the extrema of $\ell^3 S_\ell^{(0)}$ for all models occurs roughly at similar ℓ values and thus are relatively insensitive to the change in parameter B_0. We display four different values of B_0 for each model: $B_0 = 10^{-3}$ (solid), 10^{-2} (short dashed), 10^{-1} (long dashed) and 1 (dot–dashed), respectively. For HS models, we choose two different values for B_0 i.e. $B_0 = 10^{-3}$ and 10^{-2}. In agreement with what we found for optimized estimators, the skew-spectra for HS models with low n values show greater degree of sensitivity to B_0 compared to their higher n counterparts, which roughly mimic their PPF or BZ counterparts. By construction, the optimum skew-spectra are positive definite. The peak structure of the optimum estimator for a given model is different from its MFs counterparts. The odd-numbered peaks of the optimum estimator are much more pronounced compared to their even-numbered counterparts. Increasing the value of B_0 suppresses the amplitude of oscillations for both Minkowski Spectra and the optimum skew-spectra.

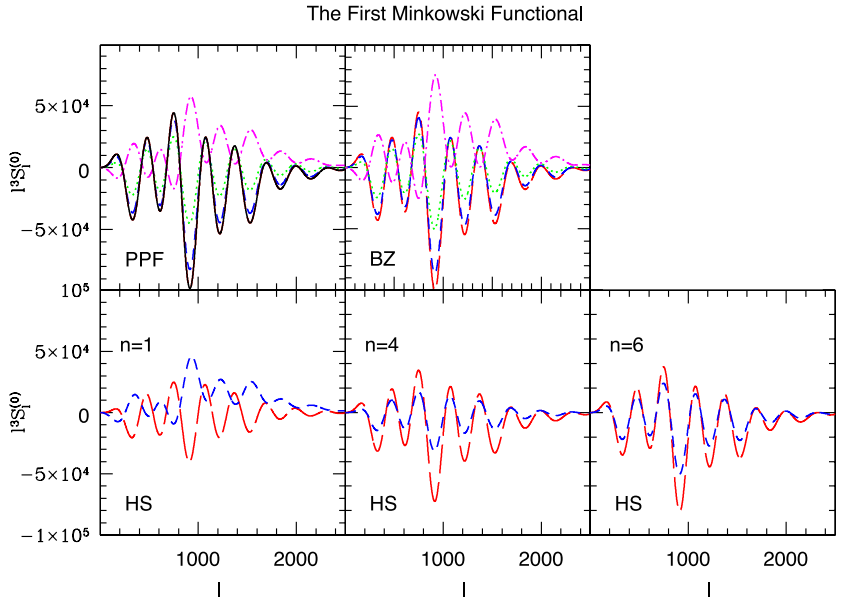

Figure 4. The first skew-spectra associated with MFs, or the first Minkowski Spectra $\ell^3 S_\ell^{(0)}$, defined in equation (29), for various theories of modified gravity, displayed as a function of the harmonic ℓ. The top-left and top-middle panels correspond to PPF and BZ, respectively. The General Relativistic prediction corresponds to $B_0 = 0$ and is shown in the top-left panel (dot and long dashed line). The bottom panels correspond to HS for $n = 1, 4, 6$, respectively. The line styles used for various models are same as Fig. 1.

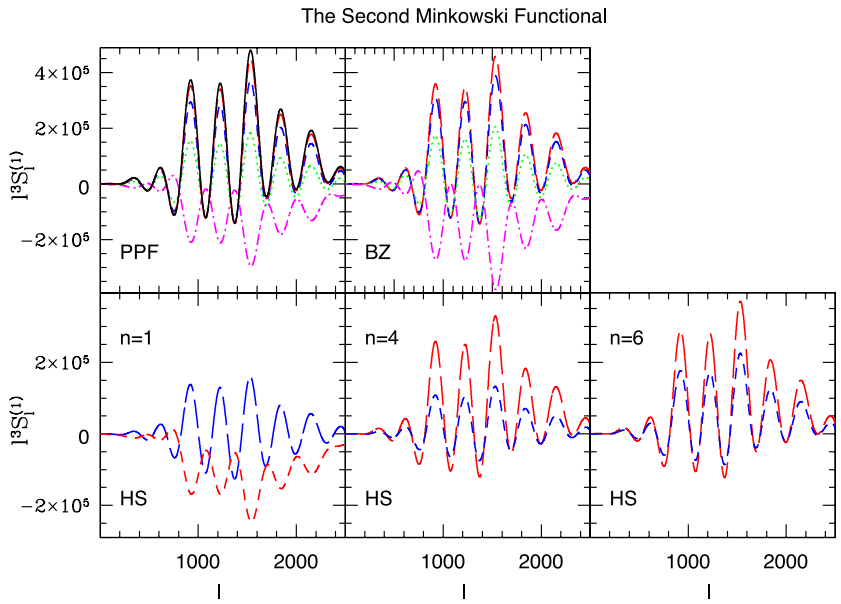

Figure 5. Same as previous figure but for the second Minkowski Spectra, i.e. $\ell^3 S_\ell^{(1)}$ defined in equation (30). The line styles used for various models are same as Fig. 1.

We have derived the covariance of the Minkowski Spectra and optimum skew-spectra. The covariance of Minkowski Spectra depends only on the ordinary temperature power spectrum and are independent of the bispectrum as they are derived in the limiting case of vanishing bispectrum. The covariance of the optimum skew-spectrum depends on the target bispectrum used for the construction of weights. Both set of covariance matrices are well conditioned. The analytical covariance matrices were derived using an all-sky approximation. The mode–mode coupling despite the all-sky approximation is related to the fact that these statistics are inherently non-Gaussian. The covariance matrices for the MFs are displayed in Fig. 7 and for the optimum skew-spectra they are displayed in Fig. 8. A comparison with results presented in Munshi & Heavens (2010) shows that we recover the terms designated as 'α' term there. The lack of corresponding 'β' terms in the current study is simply due to all-sky coverage assumed here for simplicity.

Finally, we use these covariance matrices to compute the likelihood functions. The results are obtained by using a fiducial value $B_0 = 0$. The likelihood functions of B_0 for MFs are shown in Fig. 9. The *analytical* covariance matrix for the optimum estimators is described in equation (35). These expression was used in association with equation (44) to compute the likelihood function presented in Fig. 10. In this

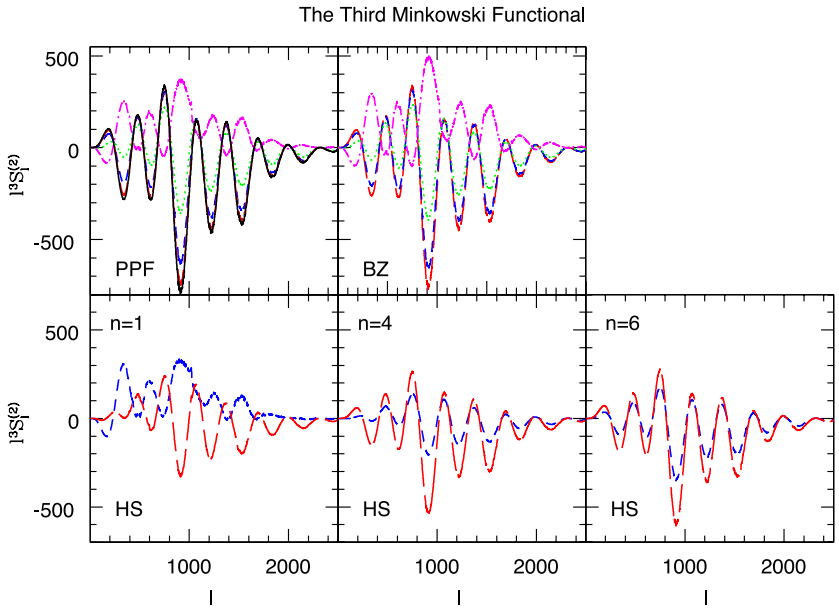

Figure 6. Same as the previous figure but for the third Minkowski Spectra $\ell^3 S_\ell^{(2)}$ defined in equation (31). The line styles used for various models are same as that of Fig. 1.

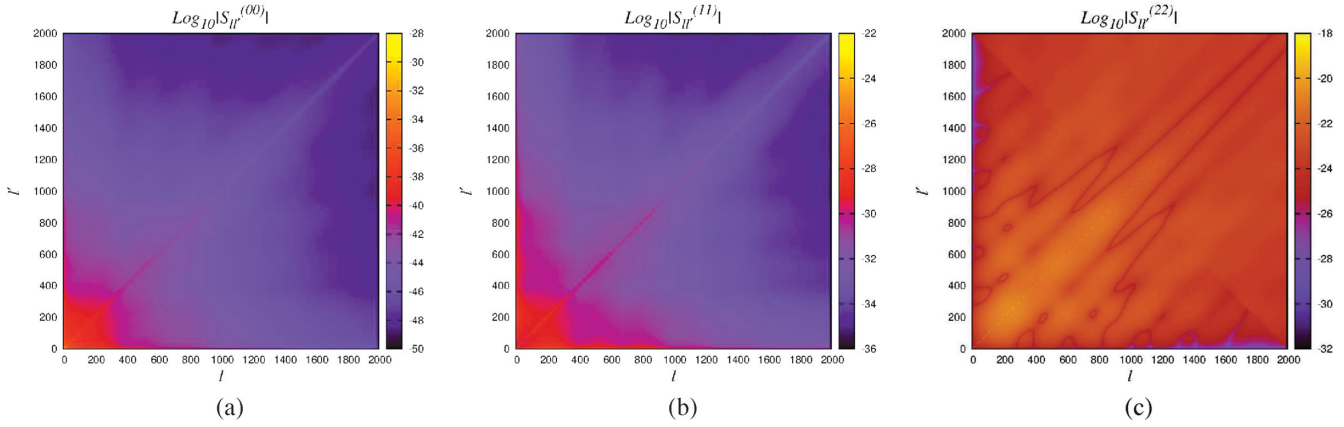

Figure 7. The all-sky covariance matrix $S_{\ell\ell'}^{(00)}$ for the estimator $S_\ell^{(0)}$ is being plotted in the left-hand panel. In middle panel, we depict $S_{\ell\ell'}^{(11)}$ and the right-hand panel corresponds to $S_{\ell\ell'}^{(22)}$. The analytical expressions for the covariance matrices are given in equation (39). For the computation of these covariance matrices, we assume $B_0 = 0$ (GR).

case, we use equation (39) for the expression of covariance matrices and in equation (43) for the expression of likelihood function. We find $B_0 < 0.67$ and $B_0 < 0.45$ for both $S_\ell^{(0)}$ and $S_\ell^{(1)}$ at 99 and 95 per cent CL, respectively. For $S_\ell^{(\rm opt)}$, the numbers are 0.071 (99 per cent CL) and 0.15 (95 per cent CL), respectively. It is important to realize that the likelihood functions are *not* Gaussian as the covariance matrices depend on B_0 in a non-trivial manner through their dependence on the CMB temperature power spectrum $\mathcal{C}_\ell^{\rm TT}$ and the lensing-temperature cross-spectrum $\mathcal{C}_\ell^{\phi \rm T}$.

7 DISCUSSION AND CONCLUSIONS

The correlation between ISW and lensing of the CMB generates a specific signature in the CMB bispectrum. Analysis of first-year data from the *Planck* satellite has detected this signature with a moderate level of signal-to-noise (S/N, 2.6σ). The ISW-lensing bispectrum is unique as it depends on the CMB power spectrum generated at recombination and cross-spectra of the lensing potential and the ISW effect generated at late times. Both ISW and lensing are sensitive to the underlying model of gravity, and thus the resulting bispectrum provides an opportunity to constrain any departure from GR. We consider various formulations of the modified gravity models which include HS, BZ and PPF models to compute the bispectrum.

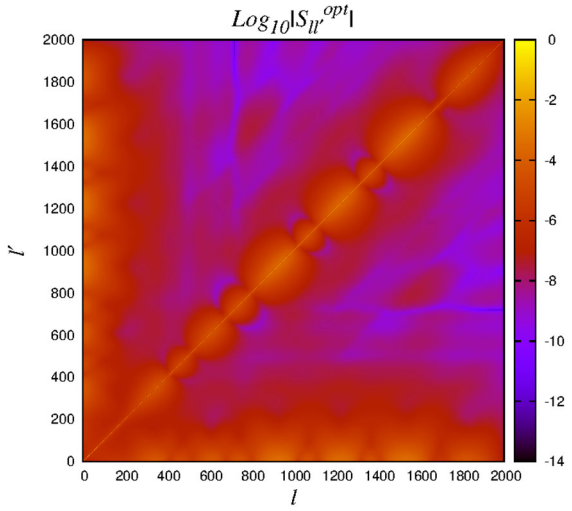

Figure 8. The all-sky covariance matrix $\mathbb{S}^{\rm opt}_{\ell\ell'}$ defined in equation (41) for the optimal estimator $S^{\rm opt}_{\ell}$ is shown. The experimental set up corresponds to *Planck* 143 GHz channel with $\ell_{\rm max} = 2000$. The mode–mode coupling, even in the case of all-sky coverage, seen here in the covariance matrix is a result of the facet that skew-spectrum is a non-Gaussian statistics. In the notation of Munshi & Heavens (2010), the covariance matrix presented here comprise of only the 'α' terms. Additional mode coupling is expected as pointed out in Munshi & Heavens (2010). The resulting 'β' terms are subdominant for near all-sky coverage. We assumed a homogeneous uncorrelated noise distribution in our calculation, see Munshi & Heavens (2010) for a complete treatment. We also assumed $B_0 = 0$ (GR) background for our computation.

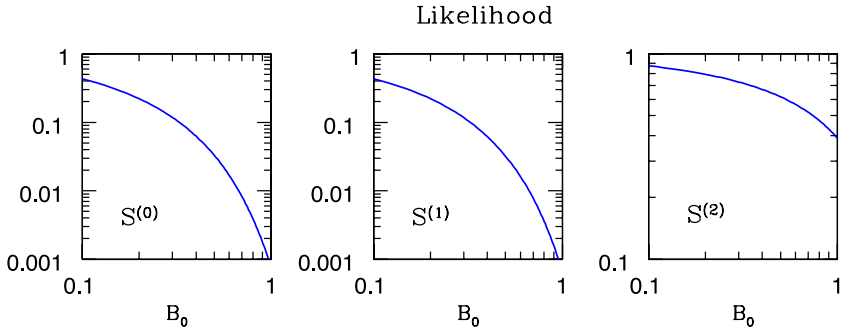

Figure 9. The likelihood functions $\mathcal{L}_{\rm S}$ defined in equation (43) for estimators $S^{(0)}_{\ell}$ (left-hand panel), $S^{(1)}_{\ell}$ (middle panel) and $S^{(2)}_{\ell}$ (right-hand panel) are plotted as a function of B_0. The parametrization used in our computation is that of BZ; primarily due to its higher speed compared to other parametrization in numerical implementation.

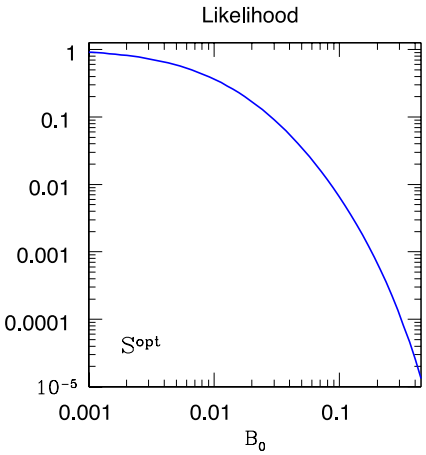

Figure 10. Likelihood for optimal estimator $S^{\rm opt}_{\ell}$ is plotted as a function of B_0 using the covariance matrix $\mathbb{S}^{\rm opt}_{\ell\ell'}$ defined in equation (41). The parametrization used in this computation is that of BZ.

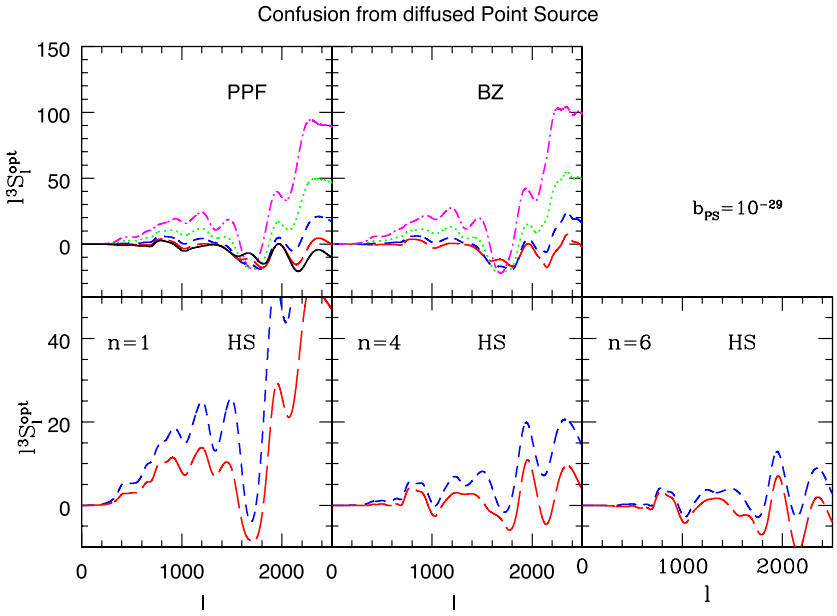

Figure 11. The confusion from unresolved PS is plotted for determination of optimum ISW-lensing skew-spectrum. The normalization for PS is fixed at $b_{\rm PS} = 10^{-29}$. The line styles used for various models are same as that of Fig. 1.

Topological estimators: the non-Gaussianity in CMB maps are often studied using moment-based approaches or alternatively using their harmonic counterparts, namely the multispectra. Extending previous results, we have studied how topological descriptors such as the MFs can provide a complementary role, paying special attention to *Planck*-type experiments. The MFs are interesting as they have different responses to various systematics. We have considered the three MFs that are used for describing the topological properties of CMB temperature maps. We compute analytically the covariance associated with the skew-spectra associated with the MFs, and our results also include cross-covariance among different skew-spectra. In agreement with previous results, we find that the skew-spectra are highly correlated. Constructing the MFs for *Planck*-type experiments (143 GHz), we find that the constraints are tighter for the first two MFs $S_\ell^{(0)}$ and $S_\ell^{(1)}$, which both give $B_0 < 0.67$ at 95 per cent CL. We do not get any meaningful constraints using $S_\ell^{(2)}$. The constraints can be further improved by considering Wiener filtering instead of Gaussian smoothing. We provide simple analytical results for the three different Wiener filtering techniques that have been considered previously in the literature. We also incorporate the optimum estimator and its covariance for construction of the corresponding likelihood. The MFs do not fare particularly well in comparison with the optimal estimators, which are predicted to give much tighter constraints: $B_0 < 0.071$ at 95 per cent CL and $B_0 < 0.15$ at 99 per cent CL. These are very close to the predictions from the full bispectrum (Hu et al. 2013b), showing their optimal nature. We have not considered the possibility of combining results from different channels which can further improve the constraints.

Contamination from PS and Galactic foregrounds: Galactic contamination are a major source of concern which can affect any study involving the CMB. They are usually dealt with masking or by using component separation techniques (Leach et al. 2008). The residual bias in the estimation of primordial non-Gaussianity was found to be small (Hikage et al. 2008a; Komatsu et al. 2011). However, other studies were more conservative in interpreting the results (Chiang et al. 2003). Techniques also exist that involve marginalizing over foregrounds (Komatsu et al. 2002, 2011). PS are an additional source of contamination for any study involving MFs. The resolved PS with sufficient S/N can be removed by application of an appropriate mask, but there will be low-flux, unresolved and unsubtracted sources, comprising radio galaxies and active galactic nuclei, that emit in radio frequencies through the synchrotron process, and dusty starburst galaxies which emit thermally. However, integrated emission from the cosmic infrared background has recently been detected by Planck Collaboration using the skew-spectrum (Planck Collaboration 2013e). Any contamination from unresolved PS can be estimated using equation (35). Some of the issues involving mask and inhomogeneous noise can be dealt with by computing the *cumulant correlators* that represent MFs in the real-space or in the *needlet* basis (Munshi et al. 2013c). The contamination from unresolved PS can be estimated using equation (35) with $X =$ ISW-lensing and $Y =$ Pointsources. The contamination is shown in Fig. 11. For normalization $b_{\rm PS} = 10^{-29}$ the contamination is several orders of magnitude lower compared to the optimum skew-spectrum depicted in Fig. 3. We have ignored the contamination from primordial non-Gaussianity which is expected to be negligible.

RS-lensing and tSZ-lensing skew-spectrum: the ISW-lensing cross-correlation at the level of bispectrum has been the focus of our study in this article. The same techniques can in principle be used to analyse skew-spectra associated with the RS-lensing or thermal SZ (tSZ)-lensing bispectrum to constrain B_0. However, the tSZ-lensing bispectrum depends on detailed modelling of underlying 'gastrophysics' and the S/N of RS-lensing skew-spectrum is below the detection threshold for ongoing surveys such as the *Planck*.

Beyond the bispectrum: the results that we have derived here are based on MFs and the optimum skew-spectrum. Going beyond third-order correlation functions, it is possible to incorporate the power spectrum of the lensing potential $C_\ell^{\phi\phi}$ in constraining B_0. Optimized

kurt-spectrum introduced in Munshi et al. (2011b) and later used to analyse 7-year data released by WMAP team (Smidt et al. 2011) can be valuable for studies in this direction. These results when combined with results from power-spectrum data alone can improve the constraints by an order of magnitude. The possibility of using polarized CMB maps will be explored elsewhere.

Constraints on B_0 *from other cosmological data sets*: constraints from CMB can provide independent confirmations of constraints derived from studies of BAOs, studies of galaxy clusters or that from weak lensing studies, though constraints from galaxy power spectrum can be significantly tighter compared to the constraints derived here, $\log_{10}B_0 < -4.07$. The scales and redshift probed by galaxy surveys and CMB observations are very different and are affected by different set of observational systematics. Hence, these observations play complimentary roles in constraining B_0.

Wiener and Wiener-like filtering and MFs: *Wiener* and *Wiener-like* filtering are generally used for analysing realistic data to confront issues related to component separation, PS and galactic masks (Ducout et al. 2013). The expressions for MFs in equations (29)–(31) can be modified by replacing the bispectrum by $\tilde{B}_{\ell_1\ell_2\ell_3} = B_{\ell_1\ell_2\ell_3} W_{\ell_1} W_{\ell_2} W_{\ell_3}$. Various forms of the filters W_ℓ that were found useful in analysing realistic data are $W_\ell^{(\mathrm{M})} = \mathcal{C}_\ell b_\ell^2/\mathcal{C}_\ell^{\mathrm{tot}}$; $W_\ell^{(\mathrm{D1})} = \sqrt{\ell(\ell+1)}\mathcal{C}_\ell b_\ell^2/\mathcal{C}_\ell^{\mathrm{tot}}$; $W_\ell^{(\mathrm{D2})} = \ell(\ell+1)\mathcal{C}_\ell b_\ell^2/\mathcal{C}_\ell^{\mathrm{tot}}$. They correspond to Wiener filtering (M) and Wiener-like filtering using first (D1) and second derivatives (D2) of the map. The expression for the covariance can be derived by replacing the power spectrum by the filtered power spectrum $\tilde{\mathcal{C}}_\ell = W_\ell^2 \mathcal{C}_\ell$ in equation (39). By definition, the optimum estimator includes inverse covariance weighting and its performance cannot be improved by filtering – inclusion of weights in the definition of optimum estimator in the numerator and denominator cancel out. As a final remark, the information content of the skew-spectrum is independent of the power spectrum, as at the lowest order the resulting cross-correlation will involve five-point spectra which vanish for a Gaussian CMB map.

ACKNOWLEDGEMENTS

DM acknowledges support through an STFC rolling grant. DM would like to thank Alexei A. Starobinsky for helpful discussions. BH and AR are indebted to Sabino Matarrese for useful discussion. BH is supported by the Dutch Foundation for Fundamental Research on Matter (FOM). AR is supported by the European Research Council under the European Community Seventh Framework Programme (FP7/2007-2013) ERC grant agreement no. 277742 Pascal.

REFERENCES

Abebe A., de la Cruz-Dombriz Á., Dunsby P. K. S., 2013, Phys. Rev. D, 88, 044050
Amendola L., Kunz M., Sapone D., 2008, J. Cosmol. Astropart. Phys., 0804, 013
Babich D., 2005, Phys. Rev. D, 72, 043003
Baker T., Ferreira P. G., Skordis C., Zuntz J., 2011, Phys. Rev. D, 84, 124018
Baker T., Ferreira P. G., Skordis C., 2013, Phys. Rev. D, 87, 024015
Bartolo N., Komatsu E., Matarrese S., Riotto A., 2004, Phys. Rep., 402, 103
Bartolo N., Bellini E., Bertacca D., Matarrese S., 2013, J. Cosmol. Astropart. Phys., 3, 34
Bean R., Tangmatitham M., 2010, Phys. Rev. D, 81, 083534
Bertacca D., Bartolo N., Matarrese S., 2011, J. Cosmol. Astropart. Phys., 08, 021
Bertschinger E., 2006, ApJ, 648, 797
Bertschinger E., Zukin P., 2008, Phys. Rev. D, 78, 024015
Bloomfield J. K., Flanagan E. E., Park M., Watson S., 2012, J. Cosmol. Astropart. Phys., 08, 010
Brax P. C., van de Bruck Davis A. C., Shaw D. J., 2008, Phys. Rev. D, 78, 104021
Brax P., Davis A. C., Li B., Winther H. A., 2012, Phys. Rev. D, 86, 044015
Calabrese E., Smidt J., Amblard A., Cooray A., Melchiorri A., Serra P., Heavens A., Munshi D., 2010, Phys. Rev. D, 81, 3529
Canavezes A. et al., 1998, MNRAS, 297, 777
Chiang L.-Y., Naselsky P. D., Verkhodanov O. V., Way M. J., 2003, ApJ, 590, L65
Clifton T., Ferreira P. G., Padilla A., Skordis C., 2012, Phys. Rep., 513, 1
Coles P., 1988, MNRAS, 234, 509
Cooray A., 2001, Phys. Rev. D, 64, 043516
Cooray A. R., Hu W., 2000, ApJ, 534, 533
Cooray A., Li C., Melchiorri A., 2008, Phys. Rev. D, 77, 103506
Daniel S. F., Linder E. V., Smith T. L., Caldwell R. R., Cooray A., Leauthaud A., Lombriser L., 2010, Phys. Rev. D, 81, 123508
De Felice A., Tsujikawa S., 2010, Living Rev. Relativ., 13, 3
Di Valentino E., Melchiorri A., Salvatelli A., Silvestri A., 2012, Phys. Rev. D, 86, 063517
Dossett J., Hu B., Parkinson D., 2014, J. Cosmol. Astropart. Phys., 03, 046
Ducout A., Bouchet F., Colombi S., Pogosyan D., Prunet S., 2013, MNRAS, 429, 2104
Eddington A. S., 1922, The Mathematical Theory of Relativity. Cambridge Univ. Press, Cambridge
Edmonds A. R., 1968, Angular Momentum in Quantum Mechanics, 2nd edn., Princeton Univ. Press, Princeton, NJ
Fang W., Hu W., Lewis A., 2008, Phys. Rev. D, 78, 087303
Ferraro S., Schmidt F., Hu W., 2011, Phys. Rev. D, 83, 063503
Giannantonio T., Martinelli M., Silvestri A., Melchiorri A., 2010, J. Cosmol. Astropart. Phys., 1004, 030
Gil-Marin H., Schmidt F., Hu W., Jimenez R., Verde L., 2011, J. Cosmol. Astropart. Phys., 1111, 019
Gleser L., Nusser A., Ciardi B., Desjacques V., 2006, MNRAS, 370, 1329
Goldberg D. M., Spergel D. N., 1999, Phys. Rev. D, 59, 103002
Gott J. R., Mellot A. L., Dickinson M., 1986, ApJ, 306, 341
Gott J. R. et al., 1989, ApJ, 340, 625

Gott J. R., Park C., Juszkiewicz R., Bies W. E., Bennett D. P., Bouchet F. R., Stebbins A., 1990, ApJ, 352, 1
Gott J. R., Mao S., Park C., Lahav O., 1992, ApJ, 385, 26
Gubitosi G., Piazza F., Vernizzi F., 2013, J. Cosmol. Astropart. Phys., 02, 032
Hadwiger H., 1959, Math. Z., 71, 124
Hall A., Bonvin C., Challinor A., 2013, Phys. Rev. D, 87, 064026
He J.-H., 2012, Phys. Rev. D, 86, 103505
Heavens A. F., Kitching T. D., Verde L., 2007, MNRAS, 380, 1029
Hikage C. et al., 2002, PASJ, 54, 707
Hikage C., Komatsu E., Matsubara T., 2006, ApJ, 653, 11
Hikage C., Coles P., Grossi M., Moscardini L., Dolag K., Branchini E., Matarrese S., 2008a, MNRAS, 385, 1613
Hikage C., Matsubara T., Coles P., Liguori M., Hansen F. K., Matarrese S., 2008b, MNRAS, 389, 1439
Hirata C. M., Ho S., Padmanabhan N., Seljak U., Bahcall N. A., 2008, Phys. Rev. D, 78, 043520
Ho S., Hirata C., Padmanabhan N., Seljak U., Bahcall N., 2008, Phys. Rev. D, 78, 043519
Hojjati A., Pogosian L., Zhao G. B., 2011, J. Cosmol. Astropart. Phys., 1108, 005
Hojjati A., Zhao G. B., Pogosian L., Silvestri A., Crittenden R., Koyama K., 2012a, Phys. Rev. D, 85, 043508
Hojjati A., Pogosian L., Silvestri A., Talbot S., 2012b, Phys. Rev. D, 86, 123503
Hu W., 2000, Phys. Rev. D, 62, 043007
Hu W., 2008, Phys. Rev. D, 77, 103524
Hu W., Sawicki I., 2007a, Phys. Rev. D, 76, 064004
Hu W., Sawicki I., 2007b, Phys. Rev. D, 76, 104043
Hu B., Liguori M., Bartolo N., Matarrese S., 2013a, Phys. Rev. D, 88, 024012
Hu B., Liguori M., Bartolo N., Matarrese S., 2013b, Phys. Rev. D, 88, 123514
Hu B., Raveri M., Frusciante N., Silvestri A., 2013c, preprint (arXiv:1312.5742)
Jain B., Zhang P., 2008, Phys. Rev. D, 78, 063503
Jennings E., Baugh C. M., Li B., Zhao G. B., Koyama K., 2012, MNRAS, 425, 2128
Kamionkowski M., Smith T. L., Heavens A., 2011, Phys. Rev. D, 83, 023007
Kerscher M., Mecke K., Schmalzing J., Beisbart C., Buchert T., Wagner H., 2001, A&A, 373, 1
Komatsu E., Wandelt B. D., Spergel D. N., Banday A. J., Gorski K. M., 2002, ApJ, 566, 19
Komatsu E. et al., 2011, ApJS, 192, 18
Laszlo I., Bean R., Kirk D., Bridle S., 2012, MNRAS, 423, 1750
Leach S. M. et al., 2008, A&A, 491, 597
Lewis A., Challinor A., Lasenby A., 2000, ApJ, 538, 473
Li B., Mota D. F., Barrow J. D., 2011, ApJ, 728, 109
Li B., Hellwing W. A., Koyama K., Zhao G. B., Jennings E., Baugh C. M., 2013, MNRAS, 428, 743
Linder E. V., 2005, Phys. Rev. D, 72, 043529
Lombriser L., Slosar A., Seljak U., Hu W., 2012, Phys. Rev. D, 85, 124038
Lombriser L., Yoo J., Koyama K., 2013, Phys. Rev. D, 87, 104019
Matsubara T., Jain B., 2001, ApJ, 552, L89
Mecke K. R., Buchert T., Wagner H., 1994, A&A, 288, 697
Melott A. L., 1990, Phys. Rep., 193, 1
Moore B. et al., 1992, MNRAS, 256, 477
Munshi D., Heavens A., 2010, MNRAS, 401, 2406
Munshi D., Melott A. L., Coles P., 2000, MNRAS, 311, 149
Munshi D., Coles P., Cooray A., Heavens A., Smidt J., 2011a, MNRAS, 410, 1295
Munshi D., Heavens A., Cooray A., Smidt J., Coles P., Serra P., 2011b, MNRAS, 412, 1993
Munshi D., Valageas P., Cooray A., Heavens A., 2011c, MNRAS, 414, 3173
Munshi D., Smidt J., Joudaki S., Coles P., 2012a, MNRAS, 419, 138
Munshi D., van Waerbeke L., Smidt J., Coles P., 2012b, MNRAS, 419, 536
Munshi D., Coles P., Heavens A., 2013a, MNRAS, 428, 2628
Munshi D., Smidt J., Joudaki S., Coles P., 2013b, MNRAS, 429, 1564
Munshi D., Smidt J., Cooray A., Renzi A., Heavens A., Coles P., 2013c, MNRAS, 434, 2830
Natoli P. et al., 2010, MNRAS, 408, 1658
Novikov D., Schmalzing J., Mukhanov V. F., 2000, A&A, 364, 17
Park C. et al., 2005, ApJ, 633, 11
Parkinson D. et al., 2012, Phys. Rev. D, 86, 103518
Perlmutter S. et al., 1999, ApJ, 517, 565
Planck Collaboration, 2013a, preprint (arXiv:1303.5062)
Planck Collaboration, 2013b, preprint (arXiv:1303.5075)
Planck Collaboration, 2013c, preprint (arXiv:1303.5077)
Planck Collaboration, 2013d, preprint (arXiv:1303.5084)
Planck Collaboration, 2013e, preprint (arXiv:1303.5079)
Pratten G., Munshi D., 2012, MNRAS, 423, 3209
Raccanelli A. et al., 2013, MNRAS, 436, 89
Reyes R., Mandelbaum R., Seljak U., Baldauf T., Gunn J. E., Lombriser L., Smith R. E., 2010, Nature, 464, 256
Riess A. G. et al., 1998, AJ, 116, 1009
Sachs R. K., Wolfe A. M., 1967, ApJ, 147, 73
Sahni V., Sathyaprakash B. S., Shandarin S. F., 1998, ApJ, 495, L5
Sato J., Takada M., Jing Y. P., Futamase T., 2001, ApJ, 551, L5

Schmalzing J., Diaferio A., 2000, MNRAS, 312, 638
Schmalzing J., Górski K. M., 1998, MNRAS, 297, 355
Schmidt F., Vikhlinin A., Hu W., 2009, Phys. Rev. D, 80, 083505
Simpson F. et al., 2013, MNRAS, 429, 2249
Smidt J., Cooray A., Amblard A., Joudaki S., Munshi D., Santos M. G., Serra P., 2011, ApJ, 728, L1
Song Y.-S., Hu W., Sawicki I., 2007a, Phys. Rev. D, 75, 044004
Song Y.-S., Peiris H., Hu W., 2007b, Phys. Rev. D, 76, 063517
Spergel D. N., Goldberg D. M., 1999, Phys. Rev. D, 59, 103001
Starobinsky A. A., 1980, Phys. Lett. B, 91, 99
Starobinsky A. A., 2007, J. Exp. Theor. Phys. Lett., 86, 157
Szapudi I., Szalay A. S., 1999, ApJ, 515, L43
Taruya A., Takada M., Hamana T., Kayo I., Futamase T., 2002, ApJ, 571, 638
Tereno I., Semboloni E., Schrabback T., 2011, A&A, 530, A68
Terukina A., Lombriser L., Yamamoto K., Bacon D., Koyama K., Nichol R. C., 2014, J. Cosmol. Astropart. Phys., 04, 013
Yamamoto K., Nakamura G., Hütsi G., Narikawa T., Sato T., 2010, Phys. Rev. D, 81, 103517
Zhang P., 2006, Phys. Rev. D, 73, 123504
Zhang P., Liguori M., Bean R., Dodelson S., 2007, Phys. Rev. Lett., 99, 141302
Zhao G. B., Pogosian L., Silvestri A., Zylberberg J., 2009a, Phys. Rev. D, 79, 083513
Zhao G. B., Pogosian L., Silvestri A., Zylberberg J., 2009b, Phys. Rev. Lett., 103, 241301
Zhao G. B., Giannantonio T., Pogosian L., Silvestri A., Bacon D. J., Koyama K., Nichol R. C., Song Y. S., 2010, Phys. Rev. D, 81, 103510
Zhao G. B., Li B., Koyama K., 2011, Phys. Rev. D, 83, 044007
Zuntz J., Baker T., Ferreira P., Skordis C., 2012, J. Cosmol. Astropart. Phys., 06, 032

This paper has been typeset from a TEX/LATEX file prepared by the author.